The 2010 IEEE/RSJ International Conference on
Intelligent Robots and Systems
October 18-22, 2010, Taipei, Taiwan

# Utilizing Compliance to Manipulate Doors with Unmodeled Constraints

Chad C. Kessens, *Student Member, IEEE,* Joseph B. Rice, *Student Member, IEEE,* Daniel C. Smith, Stephen J. Biggs, and Richard Garcia Ph.D., *Member, IEEE*

***Abstract*—Increasingly, robots are being applied to challenges in human environments such as soldier and disability assistance, household chores, and bomb disposal. To maximize a robot's capabilities within these dynamic and uncertain environments, robots must be able to manipulate objects with unknown constraints, including opening and closing doors, cabinets, and drawers. Practicality suggests that these tasks be done at or near human speed. A simple and low cost method is proposed to achieve these ends – utilizing joint compliance to resolve forces non-tangent to the path of travel. In this paper, joint compliance is achieved by means of a clutch mechanism located in line with the manipulator joint motors. When an object is to be moved, the motors are disengaged from the joints using the clutch, thus allowing the joints to move freely with the object while force is applied by the mobility platform. This enables the robot to move an object within its constraints without the need for a precise forcing vector, minimizing sensing needs as well as computation time. Other implementations of the technique are also possible, including use of inverse dynamics, back-drivable motors, and/or actively controlled slip clutches for gravity and friction compensation. The effectiveness and robustness of this approach are demonstrated through kinematic analysis, dynamic simulation, and physical experimentation on three differently sized doors and a drawer.**

## I. Introduction

While traditional applications of robotics have been limited to a very narrow scope of well-defined tasks, future demands will require robots to accomplish more complex tasks with less a priori information. Service and military robots will need to be particularly versatile [1]. They must navigate through spaces without maps, manipulate a wide range of objects without given models, and handle ever-changing, unpredictable environments with data that is often incomplete and/or inaccurate.

One major step toward achieving these goals is to manipulate objects with constraints such as those encountered and manipulated by humans every day. These objects (e.g. doors, drawers, levers, and cranks) differ from other objects (e.g. pencils and dishes) in that they are subject to narrow constraints on their motion. Whereas humans are accustomed to accommodating these constraints in real-time, they pose major challenges to robots. For example, a robot can generally manipulate a bowl into any desired pose within the robot's workspace because there are many available paths through free space. Inaccuracies along the chosen path typically have no consequence. However, when the robot attempts to manipulate a constrained object such as a door, achieving a desired object pose requires following a very specific path determined by the swing of the door. For most ground robots, application of forces that are not tangent to the path can prevent the robot from achieving the desired pose, in effect jamming the mechanism. Even small errors can potentially impart large internal forces that may damage the door, hinge, frame, manipulator, and/or mobile platform.

Whereas a variety of tasks involve constrained manipulation, one of the most useful and widely researched is door manipulation. The ability to open doors is particularly important because it greatly expands the robot's effective workspace. However, despite well over a decade of research on this problem [2], solutions remain cumbersome and relatively slow. For example, Schmid's method, which couples force/torque data with tactile data for force and position control, appears to take approximately 2 minutes to open a human door [3]. Other popular solutions such as those in [4]-[8] report manipulation times on the order of minutes or provide insufficient data on speed.

In addition, the generality and robustness of these solutions remains unclear [9]. Doors come in a variety of sizes and types, with varying weights, opening mechanisms, hinge locations, auto-closure devices, and opening directions. Typical control solutions such as those implemented in [2], [9], and [10], appear to have only been applied to doors that push open. Solutions for doors that do require pulling, such as in [11] and [12], require that the door model be known prior to opening, greatly limiting the robustness and application to the more general problem.

One method to combat these known issues is compliant control. Compliant control has been shown to decrease the failure rate of opening doors by Nagatani and Yuta in [2]. Although compliance was controlled actively and took approximately 1 minute to open the door, this work demonstrated the potential of manipulator compliance.

Schoenfeld et al. (the main inspiration for this work) leveraged this idea of compliance to construct a compliant wrist to pull a door open by simply driving away from the door [13]. This method greatly improves the speed with which the door can be opened while substantially reducing the cognitive burden on the operator, be it human or robot. However, this method has several drawbacks in its current form. 1) The wrist is relatively long, potentially reducing dexterity. 2) The gripper must slip on the handle without

Manuscript received September 15, 2009.

C. Kessens, J. Rice, S. Biggs, and R. Garcia are with Motile Robotics Inc., a contractor to the United States Army Research Lab, APG, MD 21005 USA (e-mail: chad.kessens@arl.army.mil). C. Kessens is also a Ph.D. student at the University of Maryland, College Park, MD 20742 USA.

D. Smith is an undergraduate in the Department of Computer Engineering at West Virginia University, Morgantown, WV 26507 USA.

losing contact, limiting generic application. 3) Compliance is uncontrolled, caused by a force buildup exceeding a static magnetic breaking point. Thus, forces that can be imparted by the manipulator during other activities are limited.

To combat the limitations of Schoenfeld's method and expand its usability, this paper proposes a generic, but robust approach to manipulating constrained objects. This entails utilizing joint compliance to resolve forces non-tangent to the path of travel. In this paper, joint compliance is achieved by introducing clutch mechanisms at each joint. When these clutches engage the motors, the manipulator functions normally. However, when a constrained object is to be manipulated, the clutches disengage selected motors from their joints, allowing free rotation. Therefore, the proposed approach to door opening is to drive up to the door, grasp and manipulate the handle normally (clutches engaged), then disengage the clutches, and drive away. For the purposes of exploring the solution space, the robot in this paper drives in straight line paths at varying angles. However, future work will include active course correction to increase the opening range and to handle space limitations (discussed in Section IV.A). Future work will also demonstrate the generality of the technique by utilizing inverse dynamics, backdrivable motors, and/or autonomously controlled slip clutches to achieve gravity and friction compensated compliance.

Ultimately, the goal of this work is to demonstrate the utility of the above compliance-based approach to door opening as compared with other approaches. This utility is defined in terms of five parameters: 1) opening speed, 2) computational cost, 3) robustness with respect to swing radius, 4) robustness with respect to the robot's starting position and orientation (pose) relative to the handle, and 5) robustness with respect to drive path angle. These last two points are important for two reasons. First, the approach will prove useful for lower cost robots with less precise motors and sensors. Second, the approach will be useful for opening doors in confined spaces such as at the end of a hall, on a landing, or on a side wall in a hall.

Three techniques were used to demonstrate the approach's utility. First, a numerical analysis based on the robot's inverse kinematics plotted the maximum door opening angle against the range of possible starting poses and drive angles. Second, a computer simulation analyzed the dynamic effects of the system. Finally, a physical implementation was constructed to validate the numerical results.

## II. System Overview

### A. Geometric and Mathematical Representation

To demonstrate the concept, a simple 2-D kinematic model of a robot attached to a door was developed. Important variables are defined in Table 1, and a geometric representation of the model can be found in Fig. 1. For mathematical simplicity, this model was treated as a single fixed open-chain manipulator, with its base located at the hinge of the door. The mobility platform was treated as the end effector, where it applies forces/torques to the linkage.

TABLE 1
Mathematical Variable Descriptions

| Variable | Description |
|---|---|
| X, Y | Global coordinate axes located at door hinge |
| x, y | Local coordinate axes at manipulator base |
| d | Radius (or swing) of the door |
| k | Length of the door knob |
| h | Length of the manipulator hand |
| a | Length of the manipulator arm |
| $r_1$ | Distance from hinge to arm/hand joint |
| $r_2$ | Distance from hinge to manipulator base joint |
| $\theta_1$ | Angle of door opening |
| $\theta_2$ | Angle of hand w.r.t. knob (assumed always 0) |
| $\theta_3$ | Angle of arm w.r.t. hand |
| $\theta_4$ | Angle of mobility platform w.r.t. arm |
| $\gamma$ | Angle of mobility platform w.r.t. global Y axis |
| $g_{st}(\theta)$ | Homogeneous representation of kinematic map |

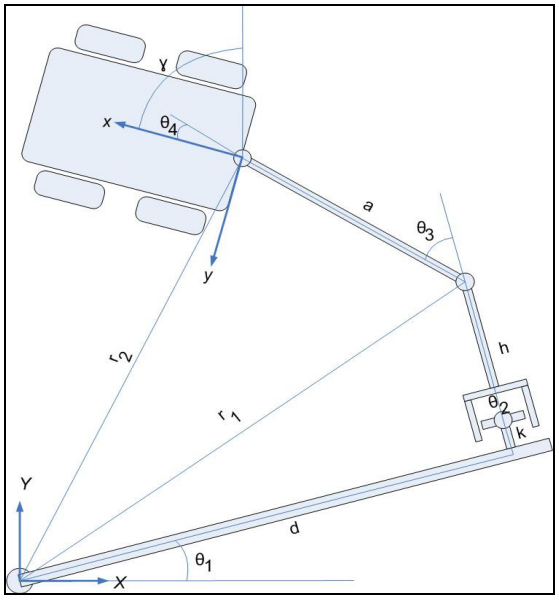


Fig. 1. Geometric model of robot. This figure provides a reference for frames, joint angles, and dimensions referred to throughout the paper.

The forward kinematics of the system could then be calculated using screw theory as outlined in [14], using variables defined in Fig. 1. First, the joint coordinates and twist axes were defined by:

$$q_1(0)=\begin{Bmatrix}0\\0\\0\end{Bmatrix},\ q_2(0)=\begin{Bmatrix}d\\k\\0\end{Bmatrix},\ q_3(0)=\begin{Bmatrix}d\\k+h\\0\end{Bmatrix},\ q_4(0)=\begin{Bmatrix}d\\k+h+a\\0\end{Bmatrix} \quad (1)$$

$$w_1=w_2=w_3=w_4=\begin{Bmatrix}0\\0\\1\end{Bmatrix} \quad (2)$$

Representing the initial configuration by:

$$g_{st}(0)=\begin{bmatrix}0&-1&0&d\\1&0&0&k+h+a\\0&0&1&0\\0&0&0&1\end{bmatrix} \quad (3)$$

yielded a forward kinematic solution:

$$g_{st}(\theta) = \begin{bmatrix} -\sin(\theta_{1234}) & -\cos(\theta_{1234}) & 0 \\ \cos(\theta_{1234}) & -\sin(\theta_{1234}) & 0 \\ 0 & 0 & 1 \\ 0 & 0 & 0 \end{bmatrix} \quad (4)$$
$$\begin{bmatrix} d\cos(\theta_1) - k\sin(\theta_1) - h\sin(\theta_{12}) - a\sin(\theta_{123}) \\ d\sin(\theta_1) + k\cos(\theta_1) + h\cos(\theta_{12}) + a\cos(\theta_{123}) \\ 0 \\ 1 \end{bmatrix}$$

where the indices in the subscript indicate the angles to be summed (e.g. $\theta_{12} \equiv \theta_1 + \theta_2$).

Because of this manipulator's simplicity, analytic inverse kinematic solutions could be found using the law of cosines. However, an infinite number of solutions exist within the workspace due to the fact that four joint variables are defined ($\theta_1$, $\theta_2$, $\theta_3$, $\theta_4$) for a 2-D system with three degrees of freedom (x, y, φ), making the system redundant. To resolve this, the goals of the project were considered, one of which was that the technique be useful to any generic end effector. Because not all end effectors are able to control slip within their grasp, a condition was imposed that $\theta_2(t) = 0$. This condition implies that slip within the end effector's grasp would not be allowed. Enforcing this condition is reasonable for the purpose of our experiment because relaxing it would actually improve the robustness of the manipulator for two reasons. First, the workspace of the system would be slightly enlarged, and second, the system would contain additional dexterity.

The inverse kinematics were then computed:

$$\theta_1 = \arctan2(x, y) - \arctan2(d, k+h) - \arccos\left(\frac{r_1^2 + r_2^2 - a^2}{2r_1 r_2}\right) \quad (5)$$

$$\theta_2 = 0 \quad (6)$$

$$\theta_3 = \pi/2 + \arctan 2(d, k+h) - \arccos\left(\frac{r_1^2 + a^2 - r_2^2}{2r_1 a}\right) \quad (7)$$

$$\theta_4 = \gamma - \theta_3 \quad (8)$$

Although two solutions exist due to mirrored dimensions, continuity of motion from the initial position was used to eliminate one of these mathematical solutions.

Using this framework, developed using the Screws and RobotLinks add-on packages for Mathematica, numerical simulations were run to determine the theoretical robustness of the proposed approach (see Section IV.A). An inverse kinematic analysis was also performed for drawer opening, but has been omitted due to space constraints.

### B. Simulation

To validate the analytical calculations and investigate dynamic effects prior to physical implementation, a computer simulation was developed. The popular physics engine ODE (Open Dynamics Engine) was selected for the simulation due to its object collision fidelity and constraint stability. ODE features a broad physics library for simulating rigid body joint constraints, collisions, and friction [15], [16], making it a well suited choice.

The door opening simulation was constructed using box and capsule primitives to create a robot, door, wall, and arm. Built-in hinge joint constraints allowed the door and arm linkages to pivot in a 2-D plane, while a built-in slider joint constrained the robot's path of motion along a specified axis. The path of the robot could be modified simply by changing the unit vector of the slider axis. To drive the robot along the desired axis, a constant force was applied to the body. Linear damping was added to ensure stability. For each starting pose and drive path angle, the force, position, and joint angle data were output by ODE's built-in rigid body functions and written to file for analysis (see Section IV.B).

### C. Hardware

To demonstrate the robustness of the concept in real-world applications and to validate the numerical models, a physical implementation was constructed. An ATRV from iRobot served as the mobility platform for the robot. It measures 0.81m x 1.16m x 0.71m (WxDxH) and utilizes skid steering as its drive method. A custom arm was attached to the rear of the ATRV such that the end-effector's height was 0.89m, near door knob height. Fig. 2 shows the physical implementation with relevant hardware labeled.

Due to desired modularity, a PR-90 rotary motor and a PW-70 2-DOF wrist motor from Schunk were selected to actuate the joints. The PR-90 was mounted to the ATRV with its rotary axis ($\theta_4$) aligned vertically. A modified caster, acting as a lazy susan bearing, attached this motor to the main beam of the arm. This mounted to a second lazy susan, and finally to the PW-70, as shown in Fig. 2. The main axis of the PW-70 ($\theta_3$) was also oriented vertically.

The distance between these two joint axes ($a$) measured 0.43m. This distance was chosen for two reasons. First, one of the most significant variables in the experiment would be the ratio of the arm length to the door radius. The doors used in experimentation had radii of 0.39m, 0.88m, and 1.78m, making the relevant ratios of $d/a$ (see Fig. 1) roughly 1, 2, and 4. Second, 0.43m is a reasonable length between these joints when compared with the equivalent projected length between joints of other robot arms stretched to doorknob height (~1.02m). These include Neuronic's Katana (0.33m) [17], Vanguard's MK2 (0.53m) [18] and iRobot's Packbot EOD Manipulator (0.55m) [19].

To gain the desired compliance, pull-type solenoids were used to lock the lazy susans in place, nominally providing the motors full control, with some minor slop. When compliance was desired, the solenoid pins were retracted, allowing the lazy susans to spin given an external wrench. A torsion spring was embedded in the lazy susan mount to return the joint to its original position, allowing the solenoid pin to relock and preserve motor encoder data. Two external tension springs were added to assist with the return. In

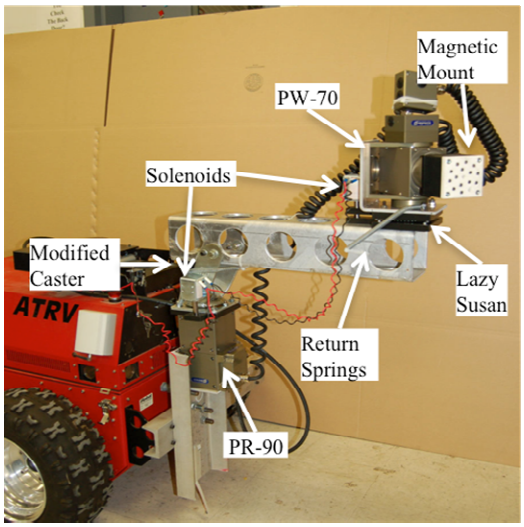

Fig. 2. Compliant manipulator mounted on I-Robot ATRV.

future designs, it is foreseen that a slip clutch mechanism will be mounted between the motor and the encoder, allowing for true position encoder data, zero slop, and no need for a return mechanism.

Finally, to enforce the rigid attachment condition ($\theta_2=0$) discussed in Section II.A and to provide a safety breakaway, a magnetic end effector was attached to the end of the PW-70 at a distance of 0.127m from the main axis. This distance was chosen based upon the wrist to fingertip lengths of the robots listed above. This was justified because the handle grasping problem lay outside the scope of this paper. To further reinforce the rigidity of the attachment, suction cups and a metal plate were attached to the doors and drawer. This attachment prevented sliding that would be inconsistent with typical end effectors. Note that a normal grasp would not require these constraints.

## III. Experimental Setup

A cabinet door ($d$=0.39m), a human-sized door ($d$=0.88m), and a large cage door ($d$=1.79m), and a drawer ($d=\infty$) were used to test the robustness of the proposed approach with respect to swing radius. First, a numerical kinematic analysis was performed to determine the maximum possible opening angle ($\theta_1$) of each door (or opening distance in the drawer case) given a starting position relative to the handle (defined by $\theta_3$) and a straight line drive path ($\gamma$). This analysis was performed at one degree intervals between 0 and 90 degrees for each parameter.

Next, dynamic simulations and physical experiments were performed to understand dynamic effects not modeled in the kinematic analysis and to validate the numerical experiments. Four starting poses for the robot were identified and marked, defined by $\theta_3$ = 0, 30, 60, and 90 degrees when the end effector "grasped" the handle. Then, for each starting pose, the robot was driven along straight line paths of $\gamma$ = 0, 30, 60, and 90 degrees. Thus, 16 simulations and 16 physical tests were performed for each object. The maximum achievable opening position of each object was used as the output metric in each test.

For each test, the following procedure was used: Given the starting pose and drive path angle, the arm motors were driven to the kinematically appropriate angles such that the robot could effectively "grasp" the handle. The robot was then oriented to the desired experimental path angle and coinciding initial position. Next, the solenoid pins were retracted, disengaging the motors from the joint motions. Then, the mobility platform was controlled remotely to run straight along its designated path, pulling on the object. Floor markings were used to verify path accuracy. Once the maximum pulling force or torque was exceeded, the object detached from the robot manipulator, and the springs rotated the joints back to their locking positions. The solenoid pins were then extended, restoring the arm to its original position and functionality. The final open position was measured and recorded. To validate the numerical results, dynamic effects were minimized by driving slowly, at a velocity of 0.02m/s. Driving at faster speeds would obviously allow the door to open much wider due to the door's angular momentum, a strategy which could prove useful in future implementations, and speed tests were performed to gauge potential opening speed. Note: In some cases, the grasp released prematurely due to insufficient torque from the magnetic grasper. For these cases, attachment was re-established and the robot was allowed to continue. Such cases were noted in the results.

## IV. Results

### A. Numerical Results

Based on the inverse kinematics described in Section II.A, numerical simulations were used to determine the maximum predicted angle to which each door could be opened for each path angle and initial position in one degree intervals. Results are shown in Fig. 3 and Fig. 4 respectively. Note that for readability, 30 degree intervals were shown for the constant parameter.

The first notable trend in the graphs is the strong dependence on path angle relative to initial position. This is clear for two reasons. First, the separation between data lines is larger between constant path lines (Fig. 3) than it is for constant initial position lines (Fig. 4). Second, the slopes of the constant path lines are flatter than the constant initial position lines.

Another notable trend is that the effect of changing the initial position decreases with increasing swing radius. This is evident from the decreasing slopes of the constant path lines (Fig. 3) as the swing radius gets larger.

The dramatic fall-off of many lines is also obvious. Generally, this occurs when the robot has moved to a location such that the pose required to maintain attachment is no longer in the manipulator's workspace. Real-time course adjustment will be necessary in these cases to keep the required pose in the manipulator's workspace. However, this is obviously a wide space. The size of the space is particularly obvious in Fig. 5, which shows the combinations of initial angles and straight-line path angles which lead to

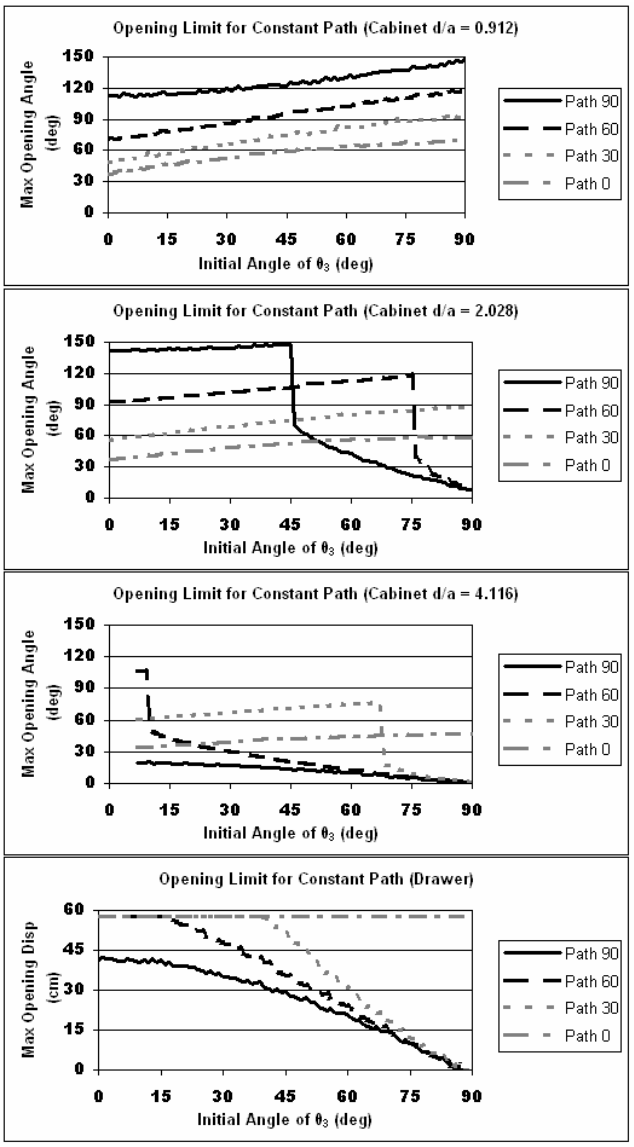


Fig. 3. Predicted results based on numerical kinematic analysis. Details the impact of varying the path angles.

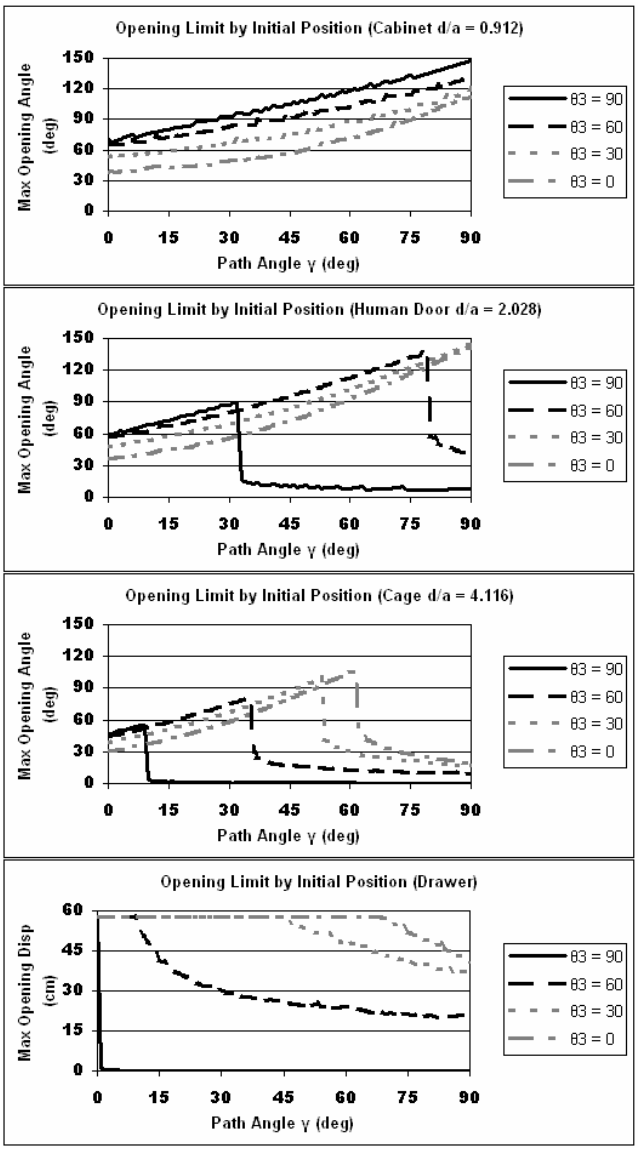


Fig. 4. Second, the slopes of the lines for constant path are smaller than those for constant initial position.

"successful" door and drawer opening positions. Here, a successful door opening angle ($\theta_{ls}$) was defined by a projected opening of 0.66m or greater, calculated by:

$$\theta_{1S} = \cos^{-1}\left(\frac{d - 0.66}{d}\right) \quad (9)$$

This would allow a robot of average width (e.g. Vanguard's MK2 (0.44m) [18], iRobot's Packbot (0.51m) [19], or Segway's RMP100 (0.61m) [20] used on Stanford's STAIR [21]) to drive straight through the doorway. It should be noted that this criterion is actually more stringent than would be absolutely necessary for passing through the door, allowing the robot to drive straight in, perpendicular to the doorway. This grants the robot a reasonable margin of error, enabling more rapid doorway navigation.

In the case of the cabinet, which is smaller than the robot, an angle of 90 degrees was used as the success criterion. For the drawer, we used a success criterion of 75% open (43.4 cm) for two reasons. First, the drawer we used had a longer

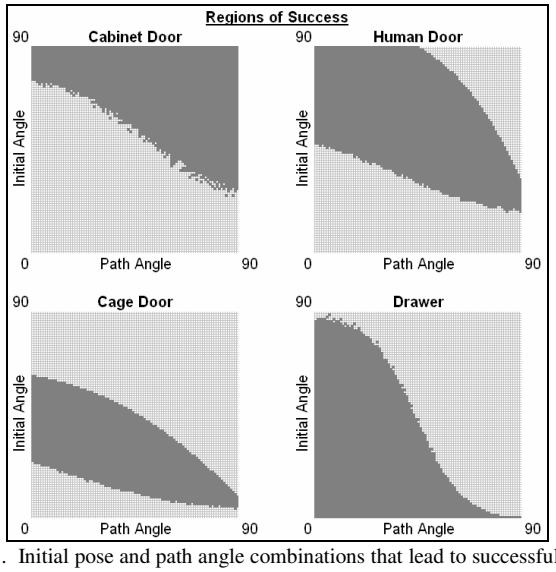


Fig. 5. Initial pose and path angle combinations that lead to successful door opening as defined by a projected opening width of 0.66m.

than normal opening distance (57.8 cm). Also, this distance should allow enough room for any object to be retrieved from the drawer. Humans rarely open a drawer all the way.

This analysis demonstrates the robustness of the technique to variations in object constraints, initial robot position, and path angle. As Fig. 5 shows, a very large number of initial pose and straight-line path combinations result in successful manipulation of the objects of interest. This is significant because it demonstrates that using this technique would allow for significant error. If coupled with modest real-time course corrections, rapid door opening seems possible even in many confined situations without much computational or sensing overhead.

### B. Simulation Results

Next, computer simulations were used to analyze dynamic effects not captured in the numerical model. The rigid body simulation actually predicted larger opening angles than the kinematic analysis, caused by the door's momentum. Once the robot reached the maximum angle, as mathematically calculated, the inertial forces of the door pulled the robot in reverse, permitting a greater door opening angle and suggesting a future strategy. Note that this strategy was used for doors that push open in [8]. This improved result is evident in the peaks of the angle oscillations in Fig. 6.

To accurately validate the mathematical data using the simulation, the measure of the maximum angle was taken at the time step where the displacement magnitude was at a maximum. Once this correction was made, the rigid body simulation nearly replicated the numerical results in Section IV.A, with a maximum deviation of 5.5 degrees (see Table 2). From Table 2, the error appears to be inversely proportional to the size of the door. This is not surprising because any error in the X-Y displacement of the door's edge will be divided by the size of the door when computing the angle according to:

$$\theta_1 = \cos^{-1}\left(\frac{X + \Delta X}{d}\right) \tag{10}$$

Thus, larger doors yield larger relative denominators for the same XY displacement error, and hence smaller angle errors.

The simulation also revealed that the size of the robot in relation to the door adds limitations to the maximum door

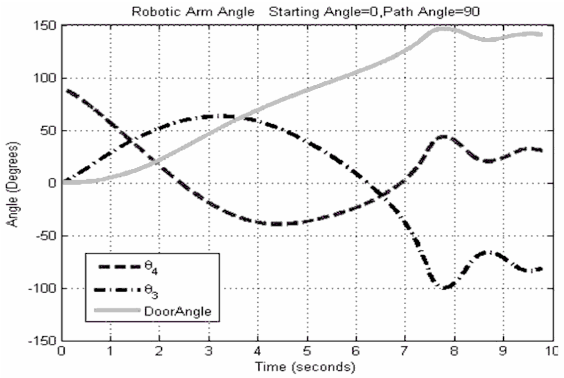


Fig. 6. Door and joint angles as a function of time. This is an example plot, specifically for the test case $\theta_3(0) = 0$, $\gamma = 90$, acting on the human door. Note the oscillatory motion at the end, showing system dynamics.

TABLE 2
Maximum Error and Standard Deviation of Simulation

| | Cabinet | Human | Cage |
|---|---|---|---|
| Max Error | 5.5° | 4.2° | 1.6° |
| Standard Deviation | 1.3° | 0.9° | 0.5° |

angle not accounted for in the kinematic analysis. At certain configurations, the door will collide with the robot as it opens, impeding the motion of door swing. Note that to obtain a more appropriate error analysis, data points that caused robot/door collisions were ignored in the comparison shown in Table 2.

### C. Experimental Results

Based on the procedures described in Section III, experimental results were obtained using a physical implementation of the proposed concept as described in Section II.C. The results of these experiments are displayed in Fig. 7.

In several experiments, the magnetic link had insufficient strength to impart the torques required to maintain rigid contact. These cases appear in light gray. In these cases, connection was reestablished, and the experiment proceeded. Both results are displayed. A firmer, more realistic grasp of the door would be able to impart larger torques than the magnetic gripper that was used, justifying the procedure.

In other instances, the tire of the mobility platform interfered with the door opening as predicted by the dynamic simulations. This restricted the opening ability by a factor

| Cabinet Door (deg) | | | | | | Error (deg) | | | |
|---|---|---|---|---|---|---|---|---|---|
| | | Initial Angle of $\theta_3$ | | | | Initial Angle of $\theta_3$ | | | |
| | | 0 | 30 | 60 | 90 | 0 | 30 | 60 | 90 |
| Path Angle | 0 | 40 | 57 | 65 | 70 | -1.1 | -3.7 | 1.0 | -2.8 |
| | 30 | 55 | 70 | 85 | 97 | -7.7 | -4.4 | -0.8 | -3.6 |
| | 60 | 77 | 90 | 105 | 120 | -5.2 | -4.7 | -1.9 | -1.1 |
| | 90 | 110 | 120 | 132 | 0* | 3.8 | -2.7 | -0.1 | 144.5* |

| Human Door (deg) | | | | | | Error (deg) | | | |
|---|---|---|---|---|---|---|---|---|---|
| | | Initial Angle of $\theta_3$ | | | | Initial Angle of $\theta_3$ | | | |
| | | 0 | 30 | 60 | 90 | 0 | 30 | 60 | 90 |
| Path Angle | 0 | 39 | 50 | 54 | 58 | -1.6 | -1.2 | 3.0 | 0.2 |
| | 30 | 59 | 70 | 82 | 5/88 | -3.0 | -0.9 | -2.0 | 84.5/1.5 |
| | 60 | 98 | 101 | 19/116 | 5 | -5.3 | 0.8 | 95.1/-1.9 | 3.4 |
| | 90 | 139 | 7.5/148 | 21/38 | 0* | 3.1 | 138.3/-2.2 | 19.6/2.6 | 8.3* |

| Cage (deg) | | | | | | Error (deg) | | | |
|---|---|---|---|---|---|---|---|---|---|
| | | Initial Angle of $\theta_3$ | | | | Initial Angle of $\theta_3$ | | | |
| | | 0 | 30 | 60 | 90 | 0 | 30 | 60 | 90 |
| Path Angle | 0 | 29 | 38 | 45 | 46 | 1.7 | 1.3 | 0.3 | 1.2 |
| | 30 | 57.5 | 64 | 70/77 | 1 | 0.8 | 3.8 | 5.4/-1.6 | 0.5 |
| | 60 | 103 | 26 | 9 | 0 | 2.5 | 4.5 | 3.7 | 1.4 |
| | 90 | 15 | 8* | 2.5* | 0* | 4.3 | 8.9* | 7.4* | 0.0* |

| Drawer (cm) | | | | | | Error (cm) | | | |
|---|---|---|---|---|---|---|---|---|---|
| | | Initial Angle of $\theta_3$ | | | | Initial Angle of $\theta_3$ | | | |
| | | 0 | 30 | 60 | 90 | 0 | 30 | 60 | 90 |
| Path Angle | 0 | 57.8 | 57.8 | 29.2/57.8 | 0.0/57.8 | 0.0 | 0.0 | 28.6/0.0 | 57.8/0.0 |
| | 30 | 39.4/57.8 | 23.5/57.8 | 8.9/27.3 | 0.0 | 18.4/0.0 | 34.3/0.0 | 16.3/-2.1 | 0.0 |
| | 60 | 25.4/57.8 | 20.3/51.4 | 5.1/22.9 | 0.0 | 31.5/-0.9 | 21.4/-9.7 | 14.4/-3.4 | 0.0 |
| | 90 | 19.1/40.6 | 16.5/34.3 | 3.8/17.8 | 0.0* | 18.4/-3.2 | 15.9/-1.9 | 11.3/-2.6 | 0.0* |

Fig. 7. Results of physical door opening tests. Left column indicates maximum opening angles and lengths based on initial position and path angle. Right column indicates error in experimental data as compared with theoretical kinematic predictions. Gray boxes indicate premature release. The left number in these boxes is the angle at which initial release occurred; the right number indicates the final angle/position achieved after reattachment. Asterisks indicate robot-door or robot-wall collisions.

not accounted for in the kinematic model. Cases where the tire interfered are indicated with an asterisk.

Overall, the experimental data matched the theoretical data fairly closely. The cabinet door provided the largest error, with a maximum of 7.7 degrees. This error can be explained in part by imperfections in the cabinet. Experiments with both the human and cage doors showed a maximum difference of less than 6 degrees between theory and experiment. These errors are most likely due to the existence of some slop in the bearings, which allowed the manipulator lengths to change somewhat. Drawer experiments similarly yielded small errors in most cases, but the grasper repeatedly became detached due to insufficient magnetic force (and thus torque). Upon detachment, the detachment was noted (see light gray regions in Fig. 5), the grasper was reattached, and the experiment continued.

Finally, several experiments were performed to determine the potential effect of the proposed method on speed. Opening speed was largely dependent on the gripper's ability to maintain a grasp of the door, as well as the acceleration and speed capabilities of the mobility platform. For our experimental setup, the proposed method was capable of fully opening a human door in approximately 4 seconds for some angles. Videos of selected speed tests were included with this paper's submission.

## V. CONCLUSIONS

Use of compliance through the addition of clutch mechanisms to manipulator arm joints enabled rapid manipulation of doors. This manipulation was robust to door radius, the robot's initial pose, and drive path angle. As a result, this method should be applicable to opening doors in confined areas such as at the end of a hall or on a side wall of a hall without great difficulty. Further, while simple, straight line paths were tested, more appropriate paths, planned in real-time using modest sensory data feedback, should improve opening angles while incurring minimal speed sacrifices. Alternative implementations of the technique will be required for fieldable implementations. These include using inverse dynamics, backdrivable motors, or actively controlled slip clutches to achieve gravity and friction compensation. Regardless of how it is achieved, the results herein demonstrate that the utilization of compliance could radically improve the speed and ease with which constrained objects are manipulated.

## ACKNOWLEDGMENT

The authors would like to thank Dr. Martin Buehler of iRobot and Mr. Jack Craft of Honeybee Robotics for their input during discussions of door opening approaches. We would also like to thank Dr. MaryAnne Fields of U.S. Army Research Laboratory and Mr. Miles Pekala of Motile Robotics Inc. for their assistance with hardware.

This work was sponsored by the U.S. Army Research Laboratory under contract number DAAB07-03-D-B010. The views and conclusions contained in this document are those of the authors and should not be interpreted as representing the official policies, either expressed or implied, of the Army Research Laboratory or the U.S. Government.

## REFERENCES

[1] Force Operating Capabilities, Pamphlet 525-66, TRADOC, Fort Monroe, VA, July 2005.

[2] K. Nagatani, S. Yuta, "An Experiment on Opening-Door-Behavior by an Autonomous Mobile Robot with a Manipulator", *IEEE/RSJ International Conference on Intelligent Robots and Systems*, 1995, vol.2, pp.45-50.

[3] A. Schmid, N. Gorges, D. Goger, H. Worn, "Opening a Door with a Humanoid Robot Using Multi-Sensory Tactile Feedback", *IEEE International Conference on Robotics and Automation*, 2008.

[4] G. Niemeyer, J. Slotine, "A Simple Strategy for Opening an Unknown Door", *IEEE International Conference on Robotics and Automation*, 1997, pp.1448-1453.

[5] L. Petersson, D. Austin, D. Kragic, "High-Level Control of a Mobile Manipulator for Door Opening", *IEEE/RSJ International Conference on Intelligent Robots and Systems*, 2000, pp.2333-2338.

[6] C. Rhee, W. Chung, M. Kim, Y. Shim, H. Lee, "Door Opening Control Using the Multi-Fingered Robotic Hand for the Indoor Service Robot", *IEEE International Conference on Robotics and Automation*, 2004, vol.4, pp.4011-4016.

[7] C. Ott, B. Baeuml, C. Borst, G. Hirzinger, "Autonomous Opening of a Door with a Mobile Manipulator: A Case Study", 6th *IFAC Symposium on Intelligent Autonomous Vehicles (IAV)*, 2007.

[8] H. Arisumi, J. R. Cardonnet, K. Yokoi, "Whole-body Motion of a Humanoid Robot for Passing Through a Door – Opening a Door by Impulsive Force," IEEE/RSJ International Conference on Intelligent Robots and Systems, 2009, pp. 428-434.

[9] A. Jain, C. Kemp, "Behaviors for Robust Door Opening and Doorway Traversal with a Force-Sensing Mobile Manipulator", *RSS Manipulation Workshop: Intelligence in Human Environments*, 2008.

[10] A. Andreopoulos, J. Tsotsos, "Active Vision for Door Localization and Door Opening using Playbot: A Computer Controlled Wheelchair for People with Mobility Impairments", *Canadian Conference on Computer and Robot Vision*, 2008, pp.3-10.

[11] J. Ohwi, S. Ulyanov, K. Yamafuji, "GA in Continuous Space and Fuzzy Classifier System for Opening a Door with Manipulator of Mobile Robot: New Benchmark of Evolutionary Intelligent Computing", *Journal of Robotics and Mechatronics*, 1995, vol.8, no.3, pp.297-301.

[12] A. Petrovskaya, A. Ng, "Probabilistic Mobile Manipulation in Dynamic Environments with Application to Opening Doors", *International Joint Conference on Artificial Intelligence*, 2007.

[13] E. Schoenfeld, L. Parrington, S. Von Muehlen, "Door Breaching Robotic Manipulator", *SPIE/Unmanned Systems Technology X Conference*, 2008, vol. 6962.

[14] R. Murray, Z. Li, S. Sastry, A Mathematical Introduction to Robotic Manipulation, CRC Press LLC, ISBN 0-8493-7981-4, 1994.

[15] A. Seugling, M. Rolin, *Evaluation of Physics Engines and Implementation of a Physics Module in a 3d-Authoring Tool*, Masters Thesis, Department of Computing Science, Umea University, 2006.

[16] A. Boeing, T. Braunl, "Evaluation of Real-Time Physics Simulation Systems", *Graphite 2007*, pp. 281-288.

[17] Katana manipulator specs. Website available: http://www.neuronics.ch/cms_en/web/index.php?id=278

[18] Vanguard MK-2 manipulator and mobility platform specs. Website available: www.rf-links.com/pdf/robot1.pdf.

[19] IRobot Packbot manipulator and mobility platform specs. Website available:http://www.irobot.com/pass.cfm?li=/filelibrary/pdfs/gi/robots/iRobot_PackBot510_EOD.pdf.

[20] Segway mobility platform specs. Website available: http://rmp.segway.com/category/rmp-100/ .

[21] E. Klingbeil, A. Saxena, A. Ng, "Learning to Open New Doors", *AAAI Robot Workshop and Exhibition*, 2008.